

NIR-absorbing poly(thieno[3,4-*b*]thiophene-2-carboxylic acid) as a polymer dye for dye-sensitized solar cells

Viswanathan S. Saji^a, KyuKwan Zong^b, Myoungho Pyo^{a,*}

^a Department of Printed Electronics Engineering, Sunchon National University, Chonnam 540-742, Republic of Korea

^b Institute of Science Education, Chonbuk National University, Chonbuk 561-756, Republic of Korea

ARTICLE INFO

Article history:

Received 7 October 2009

Received in revised form 17 February 2010

Accepted 29 March 2010

Available online 9 April 2010

Keywords:

Polymer dye

Poly(thieno[3,4-*b*]thiophene)

TiO₂ photoelectrode

Dye adsorption

NIR absorption

Dye-sensitized solar cell

ABSTRACT

Thieno[3,4-*b*]thiophene-2-carboxylic acid (TTHC) was newly synthesized and poly(thieno[3,4-*b*]thiophene-2-carboxylic acid) (PTTHC), showing NIR absorption with a low band gap of 1.0 eV, was prepared by chemical or electrochemical polymerization. Vis–NIR spectroscopic studies on PTTHC adsorption revealed that the presence of pendant carboxylic groups on a polymer chain is important to obtain highly sensitized TiO₂. The extent of PTTHC adsorption showed proportional increases as raising the adsorption temperatures, reaching saturation at the amount equivalent to a monolayer formation (this does not mean PTTHC monolayer coverage on TiO₂). Sequential treatments of TiO₂ revealed that the polymer can be adsorbed on N3-adsorbed TiO₂ without desorbing N3. The amounts of PTTHC adsorbed on N3-adsorbed TiO₂ with increasing adsorption temperatures implied that only a small fraction of polymer chains is involved in anchoring with most chain segments remaining unbound to TiO₂. The dye adsorption behaviors were further studied by FTIR, EDX, and TGA. Finally, PTTHC was applied for the preparation of panchromatic dye-sensitized solar cells. The power conversion efficiency (η) of 1.2% for PTTHC-adsorbed TiO₂ was increased to 4.3% after N3 adsorption on PTTHC-adsorbed TiO₂. Similar enhancement of η was observed after PTTHC treatment on N3-adsorbed TiO₂.

© 2010 Elsevier B.V. All rights reserved.

1. Introduction

During the last two decades, dye-sensitized solar cells (DSSC) have attracted extensive research interest as a potential alternative to Si-based photovoltaic cells, mainly due to its superior cost-effectiveness [1,2]. DSSC utilizes fast electron injection from molecular light absorbers to large band gap semiconducting nanoparticles during light illumination. Photosensitizers are subsequently recovered by obtaining electrons from redox species in an electrolyte solution for continuous current generation. One of the most crucial factors determining the overall cell performance in this type (Grätzel type) of cell is the light-harvesting capability of photosensitizers chemisorbed on the semiconducting surface. In this regard, significant efforts have been made to develop more efficient light absorbing materials especially in the near infrared (NIR) region to reach the theoretical power conversion efficiency [3,4].

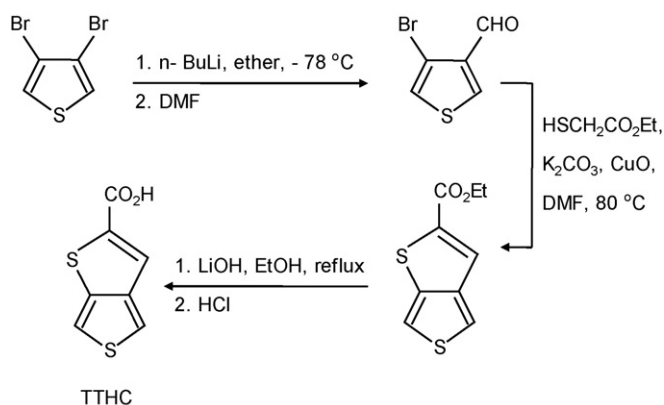
The most efficient sensitizers employed for DSSC to date are precious metal (Ru)-based dyes, including N3 dye and N719 dye, with which power conversion efficiency as high as 10% has been reported [5]. The black dye, probably the best Ru-based sensitizer reported so far, has an absorption extending into the NIR region

with a certified cell efficiency of ~11.1% [6,7]. These high conversion efficiencies made DSSC a potential candidate for commercial applications. However, the Ru-based compounds are unattractive in terms of cost, availability, and environmental friendliness [1,2].

In this regards, significant efforts have been made to find suitable alternatives to the precious metal dyes through development of common metal-containing organic dyes [8–11], metal-free organic dyes [12–19] and natural dyes [20,21]. The cell efficiency achieved using the common metal-containing organic dyes such as porphyrins [8,9] and phthalocyanines [10,11] were less than 5%. The reason for the low efficiency was attributed to dye aggregation and lack of directionality in the excited state. Metal-free dyes such as cyanine [4], hemicyanine [12], coumarin [13], indoline [14], triphenylamine [15], squaraine [16], perylene [17], and thiophene based dyes have been explored as sensitizers [18,19]. Most DSSC with these dyes yielded cell efficiencies greater than 5%, indicating that organic dyes can be substitutes (or at least supplements) of precious metal-based dyes.

As an inexpensive substitute for the precious metal dyes, conjugated polymers possess considerable importance because of their large absorption coefficients and tunable band gaps that span the whole visible and NIR region. Excluding the application of conjugated polymers as donor materials in bulk heterojunction solar cells or hole transporting layers in solid state DSSC, only a few reports are available on conjugated polymers as a sensi-

* Corresponding author. Tel.: +82 61 750 3638; fax: +82 61 750 3608.
E-mail address: mho@sunchon.ac.kr (M. Pyo).



Scheme 1. Synthetic route of TTHC.

tizer dye in the conventional DSSC [22–27]. Among conjugated polymers, polythiophene derivatives have been predominantly utilized as dye materials because of their high stability at both doped and undoped states and facile structural modifications [22,24,25,27]. For example, Yanagida et al. used poly(3-thiophene acetic acid) to produce an overall power conversion efficiency of ~2.4% [25].

In this paper, we describe the synthesis of thieno[3,4-*b*]thiophene-2-carboxylic acid (TTHC) using a novel route and poly(thieno[3,4-*b*]thiophene-2-carboxylic acid) (PTTHC). We incorporated thienothiophene blocks since poly(thieno[3,4-*b*]thiophene) has been known as one of the lowest band gap polymers having E_g of 0.85 eV [28,29]. We also expected that TTHC can be a stable derivative of unstable thieno[3,4-*b*]thiophene [30]. The adsorption behaviors of PTTHC onto nanocrystalline TiO_2 and the photovoltaic performances of the polymer-sensitized DSSC are described. Coadsorption behaviors of PTTHC and N3 are also presented.

2. Experimental

2.1. Materials

All the solvents and chemicals employed in this study, unless otherwise specified, were AR grade quality from Sigma–Aldrich. Commercial TiO_2 paste (Ti-Nanoxide T20, Solaronix SA, Switzerland) was employed for the photoelectrode fabrication. The Ru complex used was N3 (Ruthenium 535, Solaronix SA, Switzerland).

2.2. Synthesis of TTHC

Scheme 1 shows the synthesis route of TTHC. 3,4-dibromothiophene (10.0 mmol, dissolved in 25 mL ether) was stirred for 30 min at -78°C under N_2 atmosphere, followed by injection of *n*-butyllithium (10.0 mmol). After additional 30 min stirring, dimethylformamide (10.0 mmol) was dropped into the mixture. The reaction was allowed to continue for 2 h at room temperature. Dark-orange liquid obtained after ether extraction and vacuum evaporation, was subjected to column chromatography (hexane:ether = 3:1) to obtain 4-bromothiophene-3-carbaldehyde (yellow liquid, 60% yield).

To the 4-bromothiophene-3-carbaldehyde (2.615 mmol, dissolved in 25 mL of dimethylformamide), $\text{HSCH}_2\text{CO}_2\text{C}_2\text{H}_5$ (2.875 mmol), K_2CO_3 (3.923 mmol) and CuO nanopowder (0.0785 mmol) were added consecutively. The mixture was maintained at 80°C for 12 h. After ether extraction, vacuum evaporation, and column chromatography, ethylthieno[3,4-*b*]thiophene-2-carboxylate (gray powder) was obtained with 20%

yield. ^1H NMR (CDCl_3 , 400 MHz): δ = 7.61 ppm (s, 1H), 7.50 ppm (d, 1H), 7.28 ppm (d, 1H), 4.37 ppm (q, 2H), 1.34 ppm (t, 3H).

Hydrolysis of ethylester to carboxylic acid was performed by refluxing an ethanol solution containing ethylthieno[3,4-*b*]thiophene-2-carboxylate and excess amounts of LiOH for several hours. The precipitates formed by the addition of a few drops of 1.0 M HCl into the reaction mixture were washed with copious amounts of water via centrifugation. The pale pink color product (92% yield) was spectroscopically pure and used without further purification. ^1H NMR (DMSO, 400 MHz): δ = 7.70 ppm (s, 1H), 7.52 ppm (d, 1H), 7.41 ppm (d, 1H).

2.3. Polymerization of TTHC and characterization

For electrochemical characterization of PTTHC, polymer was synthesized on a Pt button electrode (geometrical area = 0.02 cm^2) in an acetonitrile (ACN) solution containing 10 mM TTHC and 50 mM tetrabutylammonium tetrafluoroborate (TBABF₄) by scanning potentials between 0 and +1.4 V (BAS CV-50W). All the potentials mentioned hereafter are referenced to Ag/AgCl (3 M KCl). For the determination of band gap of PTTHC, the polymer was electrochemically deposited on an FTO glass and absorption spectrum was obtained at a fully reduced state (JASCO V550). The band gap was also measured from a cyclic voltammogram.

For the adsorption studies, PTTHC was prepared by chemical polymerization with FeCl_3 . After adding FeCl_3 (5 mM), the ACN solution containing TTHC (10 mM) was kept stagnant at 4°C for 2 h. The solution color turned from yellow to darkish green, indicative of polymer formation. The average molecular weight (M_n) of PTTHC, determined from Gel Permeation Chromatography, was ~180,000.

2.4. Preparation of nanocrystalline TiO_2 photoanode

A doctor blade technique was employed for making TiO_2 films on FTO glass plates. Scotch tape was employed to control the thickness of coating. The coated electrodes were sintered at 450°C for 30 min, using a muffle furnace. The thickness of sintered films, measured by a surface profilometer (Nanoview 1000, Nano system), was ~8 μm .

2.5. Adsorption of PTTHC and N3 onto transparent TiO_2 electrode

The adsorption of the polymer onto TiO_2 nanocrystalline electrodes was investigated as a function of temperature. For these experiments, the TiO_2 coated FTO was immersed in a 20 mM polymer solution for 10 h. Experiments were conducted at 40, 60, and 80°C as well as room temperature (25°C). For the adsorption at elevated temperatures, the solution container was tightly closed using Teflon tape to avoid evaporation. After the adsorption, the electrodes were repeatedly washed in flowing ACN, followed by 1:1 mixture of ethanol and methanol. For the preparation of TiO_2 photoelectrodes sensitized in both Visible and NIR, N3 was also coadsorbed. The typical concentration of N3 used was 0.1 mM in ethanol.

Absorption spectra of the dye-adsorbed electrodes were measured using a UV-Vis spectrophotometer [UV 2401PC, Shimadzu]. A bare FTO was employed as the reference. TGA (SDT Q600), EDX (Bruker AXS), and FTIR (FTLA 200) analysis were performed to calculate the amount of PTTHC anchored on TiO_2 and to compare the relative composition of PTTHC to N3.

2.6. Measurement of cell efficiency

A sandwich cell was prepared using the dye-adsorbed TiO_2 electrode and Pt counter electrode. Surlyn film (SX 1170-25, Solaronix SA) with an exposed area of 0.10 cm^2 was used as the spacer

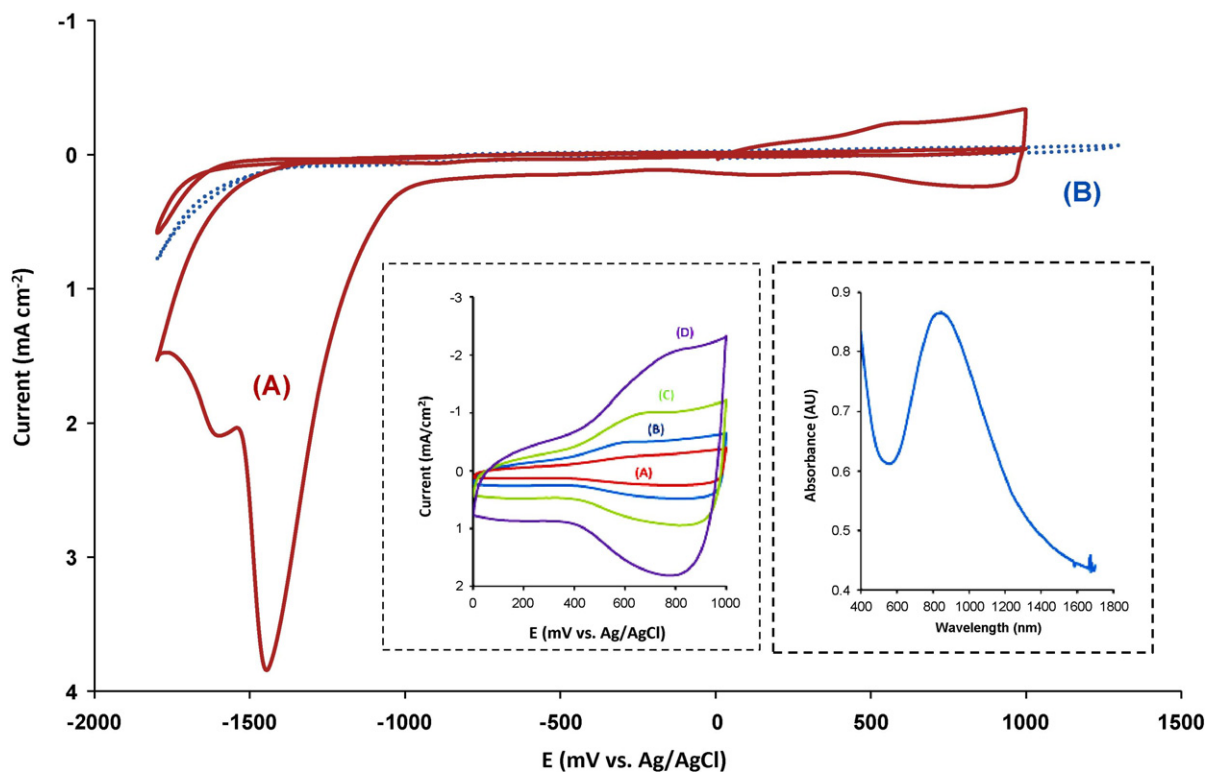


Fig. 1. Cyclic voltammograms of (A) a PTTHC-modified Pt and (B) a bare Pt in ACN containing 50 mM TBABF₄, at 50 mV s⁻¹. Inset (left): cyclic voltammograms of PTTHC-modified Pt electrode during p-doping/dedoping at (A) 50 mV s⁻¹, (B) 100 mV s⁻¹, (C) 200 mV s⁻¹, and (D) 400 mV s⁻¹. Inset (right): Vis-NIR spectrum of PTTHC in a neutral state.

between the electrodes. The photoanode together with the counter electrode was heated at 130 °C for 5 min to form a sealed cell. The iodine electrolyte was placed inside the cell utilizing capillary action through a predefined channel. A solar simulator [Newport, Model 66984] was focused to give 100 mW/cm², equivalent to 1 sun at AM 1.5G. The short circuit photocurrent (J_{sc}) and the open circuit potential (V_{oc}) were measured using a Potentiostat/Galvanostat (Epsilon EC). The counter electrode was prepared by drop-coating a propanol solution of 5 mM H₂PtCl₆ on a FTO glass. The plates were air-dried for 5 min and heated at 400 °C using a muffle furnace for 1 h. The iodide electrolyte used was comprised of 0.5 M LiI, 0.05 M I₂, and 0.5 M tert-butyl pyridine in 3-methoxy propionitrile.

3. Results and discussion

3.1. Characterization of dye

Fig. 1A represents the cyclic voltammograms (CV) recorded for the PTTHC-modified Pt electrode in ACN containing 50 mM TBABF₄. The CV was also recorded for the bare Pt electrode (Fig. 1B). While the polymer exhibits reversible p-doping processes, n-doping is quite irreversible. Once the polymer is subjected to n-doping, it immediately degrades as evidenced by the loss of electroactivity during a subsequent p-doping process. Note the huge cathodic charges during n-doping, compared to the anodic charges during p-doping. The inset (left) shows the CV of a PTTHC-modified electrode as a function of scan rate. The increase in anodic peak current with the scan rate illustrates electrochemical activity of the polymer. No substantial shift in oxidation potential was observed with the scan rate. Using the onset potential for p-doping (+0.30 V), the HOMO level of PTTHC was calculated to be -4.7 eV (vs. vacuum).

The inset (right) shows the Vis-NIR spectrum recorded for PTTHC deposited on FTO. The polymer in a neutral state at 0.0 V

exhibits an absorption peak maximum at ~820 nm with an absorption edge at 1250 nm, indicating that the band gap of the polymer is ~1.0 eV and the LUMO level lies at -3.7 eV (vs. vacuum) (PTTHC dissolved in CHCl₃ showed a similar spectrum). This value can be compared with the LUMO level electrochemically determined from the onset potential for n-doping. Note that n-doping begins at -1.0 V during the first cathodic scan, resulting in the greater band gap of 1.3 eV and the higher LUMO level at -3.4 eV (vs. vacuum) [31]. The noticeable deviation from the spectroscopically determined values may be due to the ambiguity in the determination of the onset potential, arising from significantly large cathodic charges during n-doping. This discrepancy, however, does not alter the fact that the LUMO level of PTTHC is located at the more negative potential than the conduction band of TiO₂ (-4.0 eV vs. vacuum) [32] which facilitates the charge injection from PTTHC into nanocrystalline TiO₂ of DSSC.

3.2. PTTHC adsorption onto transparent TiO₂

3.2.1. PTTHC adsorption as a function of temperature

Fig. 2 shows the transmittance spectra for the PTTHC-adsorbed TiO₂ electrodes as a function of temperature. The bare TiO₂ (Fig. 2A) exhibits substantial reduction of the transmitted lights between 400 and 600 nm due to scattering, but most of the lights were transmitted in a longer wavelength range. On the other hand, the TiO₂ electrodes treated in PTTHC solutions demonstrate gradual decreases of the transmittance with increasing temperatures (Fig. 2B–E), which is more obvious in a long wavelength range. For example, while the bare TiO₂ transmits 96% of photons at 800 nm, the transmittance of PTTHC-treated TiO₂ electrodes decreases to 93%, 88%, 70%, and 50% depending on the adsorption temperature. The greater dye loading onto TiO₂ at higher temperatures is mainly due to better solubilization of the polymer with a reduction of the aggregated phase [33].

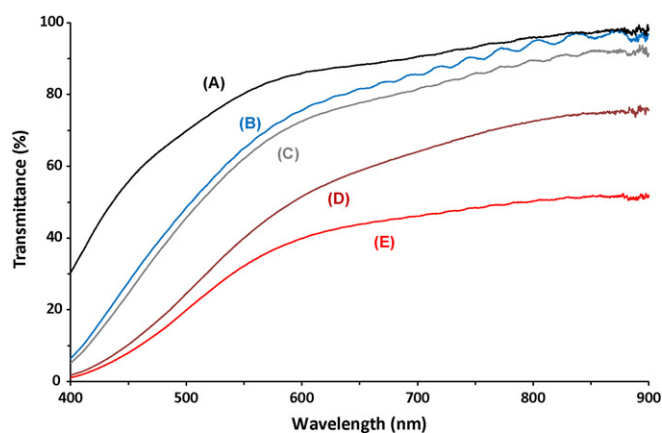


Fig. 2. Transmittance variation of PTTHC-adsorbed TiO_2 as a function of temperature: (A) bare TiO_2 ; and PTTHC-adsorbed TiO_2 at (B) room temperature, (C) 40 °C, (D) 60 °C, and (E) 80 °C.

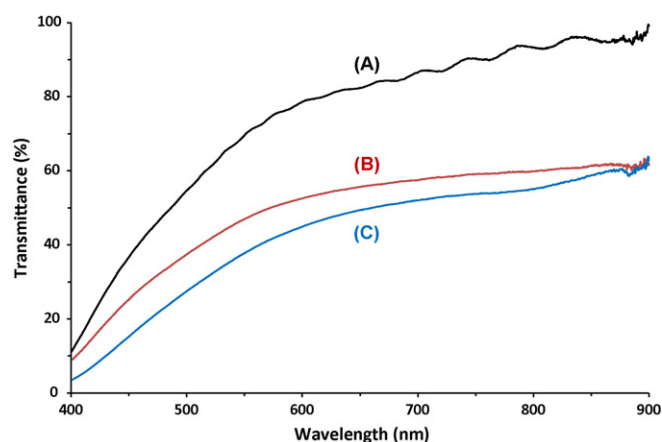


Fig. 3. Transmittance variation of (A) TTHC-adsorbed TiO_2 film; and PTTHC-adsorbed TiO_2 prepared by dipping TTHC-adsorbed TiO_2 in FeCl_3 for (B) 15 min and (C) 30 min.

We further examined two alternative methods to establish a controllable polymer adsorption method at room temperature. First, we synthesized PTTHC with TiO_2 dipped in a polymerization medium for 10 h, expecting more efficient dye adsorption at room temperature (the TiO_2 electrodes were immersed in a TTHC solution and polymerization was achieved by in situ addition of FeCl_3 to the monomer solution for 10 h). The subsequent Vis–NIR analysis showed the similar spectrum as Fig. 2B (data not shown here). This implies that the adsorption onto TiO_2 in a polymerization medium occurs mostly with the polymer, since the polymerization reaction proceeds fast at room temperature. Second, we anchored TTHC by dipping TiO_2 in a 10 mM monomer solution for 10 h and subsequently polymerized the surface-bound TTHC in a FeCl_3 solution at room temperature (the monomer-adsorbed electrodes were directly dipped into a FeCl_3 solution). Fig. 3 exhibits the transmittance spectra of the photoelectrodes before and after the surface-bound TTHC polymerization. While the transmittance of the monomer-adsorbed TiO_2 (Fig. 3A) is comparable to that of the bare TiO_2 (Fig. 2A), polymerization significantly alters the transmittance in between 600 and 900 nm due to the NIR absorption of PTTHC (Fig. 3B and C). The effect of polymerization time on transmittance is negligible, implying that the polymerization rate is quite fast and 30 min is enough for the completion of polymerization (further increase of immersion time did not result in any major variations). It is worthwhile to note that Figs. 3C and 2E show similar transmittance values. This

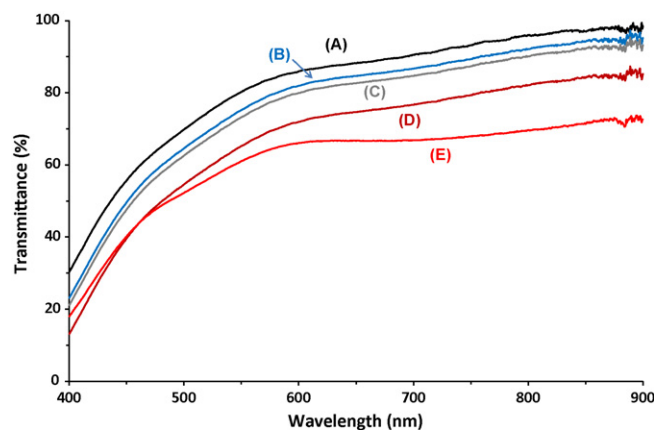


Fig. 4. Transmittance variation of the ethylester-functionalized PTTHC-adsorbed TiO_2 as a function of temperature: (A) bare TiO_2 ; and ethylester-functionalized PTTHC-adsorbed TiO_2 at (B) room temperature, (C) 40 °C, (D) 60 °C, and (E) 80 °C.

is interesting since post-polymerization after monomer adsorption should lead to the monolayer formation on the TiO_2 surface, avoiding possible problems associated with the polymer aggregation. The similar transmittance values (Figs. 3C and 2E) seem to indicate that the difference in the amounts of polymer adsorbed on TiO_2 is negligible. However, this does not necessarily mean that the surface-bound TTHC polymerization method result in a PTTHC monolayer formation. We believe that a significant fraction of PTTHC chains exists without anchoring (see below), remaining free TiO_2 surfaces which are accessible by other dyes with small molecular weights.

3.2.2. Nature of anchoring

It is well known that the carboxylic acid group is crucial for efficient dye adsorption on TiO_2 [2,34]. To confirm whether the COOH group is solely responsible for the PTTHC adsorption, we carried out Vis–NIR investigation with an ethylester-functionalized PTTHC which does not have free COOH moieties. Fig. 4 shows the transmittance spectra of TiO_2 treated in ethylester-functionalized PTTHC solutions at various temperatures. As in the case of PTTHC, the transmittance steadily decreases with the increase of temperatures and finally reaches ~70% at 80 °C. This indicates that a certain extent of dye adsorption can happen on the TiO_2 surface even in the absence of COOH groups. However, it should be noted that the extent of PTTHC adsorption at 80 °C (Fig. 2E) is significantly higher when compared with the ethylester-functionalized PTTHC (Fig. 4E). From these results, it can be concluded that the adsorption occurs more effectively through the COOH group although transesterification can occur between TiO_2 and ester-functionalized dyes to some extents.

To confirm the nature of PTTHC adsorption, we also conducted FTIR studies with the powders scratched from the dye-adsorbed photoelectrode. The FTIR peaks matched well with the characteristic peaks of neat PTTHC except COOH intensities. The peak intensities corresponding to the COOH group (1692 and 1408 cm^{-1}) significantly decreased after the dye adsorption, but were not suppressed completely. Such an observation supports that substantial amounts of carboxylic acids remain intact without being involved in the chemical linkage with TiO_2 as mentioned above.

In order to quantitatively measure the amount of polymer adsorbed at 80 °C, thermal analysis of PTTHC-adsorbed TiO_2 was performed (Fig. 5). Since TiO_2 was stable within the temperature range examined (Fig. 5A), the weight loss between 200 and 400 °C resulted from the polymer decomposition. By using the total weight loss of the polymer-adsorbed TiO_2 powder between 200 and 400 °C (~5%), the total polymer adsorbed on TiO_2 was calculated to be

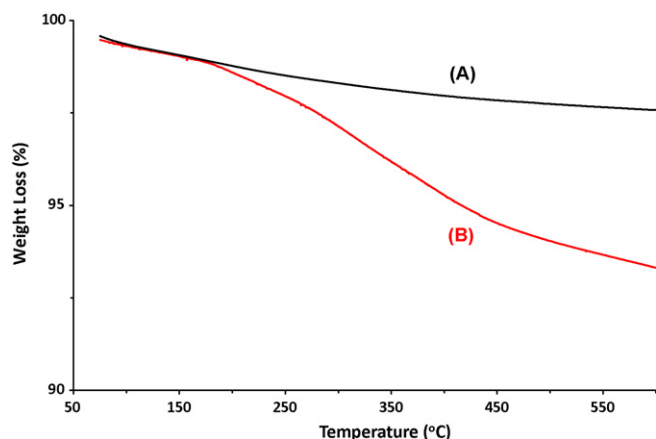


Fig. 5. Thermogravimetric analysis of (A) TiO_2 and (B) PTTHC-adsorbed TiO_2 at 80°C . $\nu = 10^\circ\text{C min}^{-1}$ under N_2 atmosphere.

~ 10 mg. With the densities of PTTHC ($\sim 1.2 \text{ g cm}^{-3}$, measured by a floatation method) and TiO_2 (4.2 g cm^{-3}), an approximate thickness of polymer on a single TiO_2 particle was calculated to be 12 Å. This value seems to be consistent with the monolayer thickness, implying that the amount of PTTHC-adsorbed on TiO_2 is equivalent to the one for the monolayer formation. Here the TiO_2 particle is assumed to be a sphere with a diameter of 20 nm.

To further confirm the amounts of dye, PTTHC was desorbed by immersing PTTHC-adsorbed TiO_2 in a 0.1 M sodium hydroxide aqueous solution for 30 min [35]. The concentration of the dye desorbed was determined by Vis-NIR spectroscopy ($\epsilon = 5.2 \times 10^3 \text{ M}^{-1} \text{ cm}^{-1}$). The thickness of polymer was calculated to be 9.5 Å, similar to the value determined from the thermal analysis.

3.3. Coadsorption of PTTHC and N3 on transparent TiO_2

Since PTTHC adsorption can allow other materials to access toward TiO_2 surfaces due to polymer chain flexibility, coadsorption of low molecular weight dyes on bare TiO_2 surfaces may widen the absorption window. In a recent report, Ogura et al. showed that a combination of black dye and indoline dye possesses a synergistic effect that improves the cell efficiency [36]. In this context, we sequentially treated TiO_2 electrodes in PTTHC and N3 to investigate coadsorption behaviors. In the first set of experiments, TiO_2 electrodes were immersed in PTTHC solutions at various temperatures for 10 h, taken out, washed thoroughly, and immersed in 0.1 mM N3 dye at room temperature for 10 h. The corresponding Vis-NIR spectra are shown in Fig. 6. The increase in absorbance between 700 and 900 nm with the increase of temperatures is also the case, as expected. Note that the absorption between 600 and 900 nm in Fig. 6 is identical to the value shown in Fig. 2E (50% transmittance is equal to the absorbance of 0.3), supporting the fact that no desorption of PTTHC occurs during N3 adsorption. The spectra also exhibit the distinctive peaks at 540 nm indicative of the N3 dye absorption. However, areas under the N3 peaks got smaller with the increase of PTTHC adsorption temperatures. This variation indicates that free TiO_2 sites accessible by N3 become smaller as the polymer adsorption increases. N3 adsorption on PTTHC-adsorbed TiO_2 is possible since only a certain portion of COOH groups is involved in anchoring.

In the second set of experiments, the above process was reversed. The TiO_2 electrodes were first immersed in N3 at room temperature for 10 h, followed by immersion in PTTHC at different temperatures for 10 h (Fig. 7). The figure indicates that the peak areas due to N3 adsorption remain constant while the absorption in

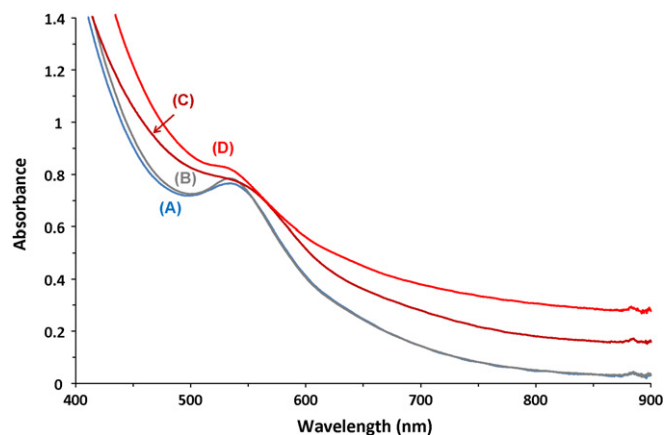


Fig. 6. Vis-NIR spectra of TiO_2 film after dipping PTTHC-adsorbed TiO_2 in a N3 solution at room temperature. PTTHC was adsorbed at (A) room temperature, (B) 40°C , (C) 60°C , and (D) 80°C .

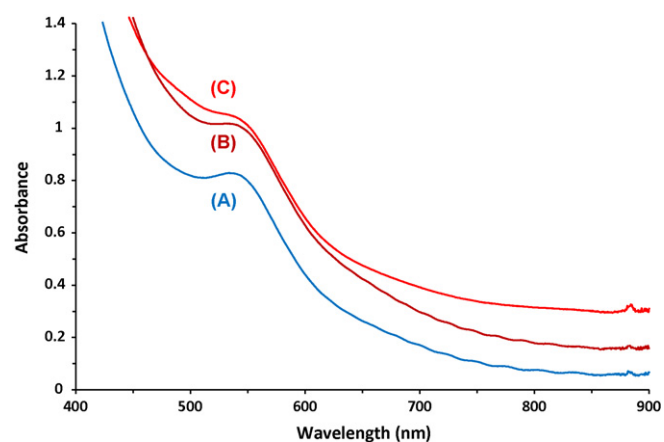


Fig. 7. Vis-NIR spectra of TiO_2 film after dipping N3-adsorbed TiO_2 in a PTTHC solution at (A) room temperature, (B) 60°C , and (C) 80°C . N3 was adsorbed at room temperature.

Table 1

EDX analysis of selected areas of dye-adsorbed TiO_2 electrodes: (A) PTTHC adsorption at 80°C , followed by N3 adsorption; (B) N3 adsorption followed by PTTHC adsorption at 80°C .

Sample	Elements/atomic (%)				
	C	S	Ti	Ru	O
A	2.79	1.37 (3.56)	38.46 (100)	0.25 (0.65)	57.13
B	2.85	1.28 (3.52)	36.35 (100)	0.28 (0.77)	59.24

the wavelength range of 700–900 nm is enhanced with the increase of PTTHC adsorption temperatures. The insignificant change of N3 peaks is not surprising since the large binding constant between carboxylic groups and titania can effectively protect N3 from desorption [37]. The increase of PTTHC adsorption with temperature is rather interesting. Since it has been known that the coverage of the TiO_2 surface with N3 reaches near 100% [38], the increase of polymer adsorption with temperature necessarily indicates that only a small fraction of polymer chains is anchored to TiO_2 and most segments exist in an unbound state.

Table 1 represents the elemental analysis by EDX for the selected areas of the dye-adsorbed electrode surface. The percentages of S and Ru reflect the amounts of PTTHC and N3 dye, respectively. It is clear that PTTHC adsorption followed by N3 adsorption (sample A) shows slightly less Ru content than N3 adsorption followed by PTTHC adsorption (sample B), while maintaining similar S contents.

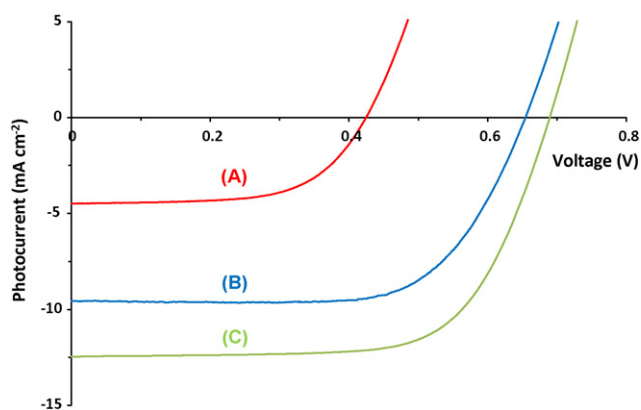


Fig. 8. J - V curves recorded for DSSC constructed using TiO_2 electrodes sensitized with (A) PTTHC, (B) PTTHC followed by N3, and (C) N3.

Table 2

Cell parameters of PTTHC and mixed-dye DSSC.

Sample	J_{sc} (mA cm^{-2})	V_{oc} (V)	FF	η (%)
PTTHC	4.5	0.42	0.62	1.2
PTTHC + N3	9.6	0.62	0.71	4.3

This corresponds to the result obtained from Vis-NIR studies (the absorbance of N3 in Fig. 6D was smaller than in Fig. 7C while the PTTHC absorbance was similar). The table also shows significantly large amounts of S relative to Ru content in both cases. Considering that the amount of PTTHC adsorbed at 80°C is equivalent to the amount for the monolayer formation and PTTHC is not desorbed during N3 treatment (for sample A), abnormally large S contents imply that PTTHC is non-specifically bound to TiO_2 along with a large portion of movable chain segments.

3.4. Photovoltaic studies

Fig. 8 represents current-voltage characteristics of DSSC prepared with PTTHC and PTTHC+N3 (PTTHC adsorption followed by N3 treatment). Table 2 lists the photovoltaic data. DSSC constructed using the polymer dye exhibited a cell efficiency of 1.2%. The efficiency increased to 4.3% when the polymer adsorption was followed by N3 treatment (N3 adsorption followed by PTTHC gave a similar η). The relatively low J_{sc} of the polymer dye DSSC may be associated with the loosely bound polymers, which prevent the electrolyte diffusion and/or electron transfer from electrolytes to dye molecules to some extents (the low V_{oc} is due to the high HOMO level of PTTHC than that of N3). The pure N3 dye-sensitized DSSC showed an efficiency of 5.8% in this study. Although η of the polymer dye DSSC and the mixed-dye-sensitized DSSC were limited, the efficiency values obtained in this study suggests that PTTHC can play a role in NIR sensitization or can be utilized for the reduction of precious metal-based dye consumption. More studies are in progress to alleviate the polymer chain stacking (or aggregation) by employing suitable co-adsorbents and by controlling the molecular weight of the polymer for further improvement of the cell efficiency.

4. Conclusions

A new monomer TTHC and a polymer PTTHC having a low band gap of 1.0 eV were synthesized. Their adsorption and NIR sensitization behaviors on TiO_2 were investigated, expecting potential application in DSSC. The result of Vis-NIR experiments showed that the extent of polymer adsorption on nanocrystalline TiO_2 was significantly enhanced with the increase of adsorption temperatures.

Comparative studies with an ethylester-functionalized polymer indicated that the COOH groups mainly contributed to dye anchoring. The FTIR and coadsorption studies revealed that the entire polymer chains were not necessarily involved in the adsorption process and only a small fraction of polymer chains was responsible for anchoring. The DSSC sensitized with PTTHC showed a cell efficiency of 1.2%, suggesting that PTTHC was involved in the NIR solar energy conversion process. Coadsorption of N3 with PTTHC resulted in an efficiency of 4.3%, which was lower than 5.8% of DSSC with N3 only. This is likely because polymer stacking (or aggregation) hampers the dye regeneration by accepting electrons from iodide electrolytes.

Acknowledgement

This research has been supported by the WCU program at Suncheon National University.

References

- [1] B. O'Regan, M. Grätzel, A low-cost, high-efficiency solar cell based on dye-sensitized colloidal TiO_2 films, *Nature* 353 (1991) 737–739.
- [2] A. Hagfeldt, M. Grätzel, Molecular photovoltaics, *Acc. Chem. Res.* 33 (2000) 269–277.
- [3] A. Burke, L. Schmidt-Mende, S. Ito, M. Grätzel, Novel blue dye for near-IR 'dye-sensitized' solar cell applications, *Chem. Commun.* (2007) 234–236.
- [4] T. Ono, T. Yamaguchi, H. Arakawa, Study on dye sensitized solar cell using novel infrared dye, *Sol. Energy Mater. Sol. Cells* 93 (2009) 831–835.
- [5] M.K. Nazeeruddin, A. Kay, I. Rodico, R. Humphry-Baker, E. Mueller, P. Liska, N. Vlachopoulos, M. Grätzel, Conversion of light to electricity by cis-X2bis(2,2'-bipyridyl)-4,4'-dicarboxylate)ruthenium(II) charge-transfer sensitizers ($\text{X} = \text{Cl}^-$, Br^- , I^- , CN^- , and SCN^-) on nanocrystalline titanium dioxide electrodes, *J. Am. Chem. Soc.* 115 (1993) 6382–6390.
- [6] M.K. Nazeeruddin, P. Péchy, T. Renouard, S.M. Zakeeruddin, R. Humphry-Baker, P. Comte, P. Liska, L. Cevey, E. Costa, V. Shklover, L. Spiccia, G.B. Deacon, C.A. Bignozzi, M. Grätzel, Engineering of efficient panchromatic sensitizers for nanocrystalline TiO_2 based solar cells, *J. Am. Chem. Soc.* 123 (2001) 1613–1624.
- [7] Y. Chiba, A. Islam, Y. Watanabe, R. Komiya, N. Koide, L. Han, Dye-sensitized solar cells with conversion efficiency of 11.1%, *Jpn. J. Appl. Phys.* 45 (2006) L638–640.
- [8] S. Hayashi, Y. Matsubara, S. Eu, H. Hayashi, T. Umeyama, Y. Matano, H. Imahori, Fused five-membered porphyrin for dye sensitized solar cells, *Chem. Lett.* 37 (2008) 846–847.
- [9] W.M. Campbell, K.W. Jolley, P. Wagner, K. Wagner, P.J. Walsh, K.C. Gordon, L. Schmidt-Mende, M.K. Nazeeruddin, Q. Wang, M. Grätzel, D.L. Officer, Highly efficient porphyrin sensitizers for dye sensitized solar cells, *J. Phys. Chem. C* 111 (2007) 11760–11762.
- [10] J. He, G. Benkö, F. Korodi, T. Polivka, R. Lomoth, B. Akermark, L. Sun, A. Hagfeldt, V. Sundström, Modified phthalocyanines for efficient NIR sensitization of nanostructured TiO_2 electrode, *J. Am. Chem. Soc.* 124 (2002) 4922–4932.
- [11] L. Giribabu, Ch.V. Kumar, V.G. Reddy, P.Y. Reddy, Ch.S. Rao, S.R. Jang, J.Y. Yum, M.K. Nazeeruddin, M. Grätzel, Unsymmetrical alkoxy zinc phthalocyanine for sensitization of nanocrystalline TiO_2 electrode, *Sol. Energy Mater. Sol. Cells* 91 (2007) 1611–1617.
- [12] Z.S. Wang, F.Y. Li, C.H. Huang, Photocurrent enhancement of hemicyanine dyes containing RSO_3^- group through treating TiO_2 films with hydrochloric acid, *J. Phys. Chem. B* 105 (2001) 9210–9217.
- [13] K. Hara, Y. Tachibana, Y. Ohga, A. Shinpo, S. Suga, K. Syama, H. Sugihara, H. Arakawa, Dye sensitized nanocrystalline TiO_2 solar cells based on novel coumarin dyes, *Sol. Energy Mater. Sol. Cells* 77 (2003) 89–103.
- [14] S. Ito, H. Miura, S. Uchida, M. Takata, K. Sumioka, P. Liska, P. Comte, P. Péchy, M. Grätzel, High conversion efficiency organic DSSC with a novel indoline dye, *Chem. Commun.* (2008) 5194–5196.
- [15] P. Shen, Y. Liu, X. Huang, B. Zhao, N. Xiang, J. Fei, L. Liu, X. Wang, H. Huang, S. Tan, Efficient triphenylamine dyes for solar cells: Effects of alkyl-substituents and π -conjugated thiophene unit, *Dyes Pigment* 83 (2009) 187–197.
- [16] J.H. Yum, P. Walter, S. Huber, D. Rentsch, T. Geiger, F. Nuesch, F. De Angelis, M. Grätzel, M.K. Nazeeruddin, Efficient far red sensitization of nanocrystalline TiO_2 film by an unsymmetrical squaraine dye, *J. Am. Chem. Soc.* 129 (2007) 10320–10321.
- [17] S. Ferrere, A. Zaban, B.A. Gregg, Dye sensitization of nanocrystalline tin oxide by perylene derivatives, *J. Phys. Chem. B* 101 (1997) 4490–4493.
- [18] S.L. Li, K.J. Jiang, K.F. Shao, L.M. Yang, Novel organic dyes for efficient dye sensitized solar cells, *Chem. Commun.* (2006) 2792–2794.
- [19] M. Xu, R. Li, N. Pootrakulchote, D. Shi, J. Guo, Z. Yi, S.M. Zakeeruddin, M. Grätzel, P. Wang, Energy levels and molecular engineering of organic D- π -A sensitizers in dye sensitized solar cells, *J. Phys. Chem. C* 112 (2008) 19770–19776.
- [20] N.J. Cherepy, G.P. Smestad, M. Grätzel, J.Z. Zhang, Ultrafast electron injection: implications for a photoelectrochemical cell utilizing an anthocyanin dye

- sensitized TiO₂ nanocrystalline electrode, *J. Phys. Chem. B* 101 (1997) 9342–9351.
- [21] B.-Q. Liu, X.-P. Zhao, W. Luo, The synergistic effect of two photosynthetic pigments in dye-sensitized mesoporous TiO₂ solar cells, *Dyes Pigment* 76 (2008) 327–331.
- [22] J.K. Mwaure, X. Zhao, H. Jiang, K.S. Schanze, J.R. Reynolds, Spectral broadening in nanocrystalline TiO₂ solar cells based on poly(*p*-phenylene ethynylene) and polythiophene sensitizers, *Chem. Mater.* 18 (2006) 6109–6111.
- [23] H. Jiang, X. Zhao, A.H. Shelton, S.H. Lee, J.R. Reynolds, K.S. Schanze, Variable-band-gap poly(arylene ethynylene) conjugated polyelectrolytes adsorbed on nanocrystalline TiO₂: photocurrent efficiency as a function of the band gap, *Appl. Mater. Interf.* 1 (2009) 381–387.
- [24] Y.G. Kim, J. Walker, L.A. Samuelson, J. Kumar, Efficient light harvesting polymers for nanocrystalline TiO₂ photovoltaic cells, *Nano Lett.* 3 (2003) 523–525.
- [25] S. Yanagida, G.K.R. Senadeera, N. Nakamura, Y. Wada, Polythiophene sensitized TiO₂ solar cells, *J. Photochem. Photobiol. A* 166 (2004) 75–80.
- [26] X. Liu, R. Zhu, Y. Zhang, B. Liu, S. Ramakrishna, Anionic benzothiadiazole containing polyfluorene and oligofluorene as organic sensitizers for dye-sensitized solar cells, *Chem. Commun.* (2008) 3789–3791.
- [27] G.K.R. Senadeera, K. Nakamura, T. Kitamura, Y. Wada, S. Yanagida, Fabrication of highly efficient polythiophene-sensitized metal oxide photovoltaic cells, *Appl. Phys. Lett.* 83 (2003) 5470–5472.
- [28] S.Y. Hong, D.S. Marynick, Understanding the conformational stability of and electronic structures of modified polymers based on polythiophene, *Macromolecules* 25 (1992) 4652–4657.
- [29] V. Seshadri, G.A. Sotzing, Polymerization of two unsymmetrical isomeric monomers based on thieno[3,4-*b*]thiophene containing cyanovinylene spacers, *Chem. Mater.* 16 (2004) 5644–5649.
- [30] G. Buemi, Molecular and electronic structures of thieno[3,4-*b*]thiophene-2-carboxylic acid and acetic thieno[3,4-*b*]thiophene-2-carboxylic anhydride. An AMI, MNDC and CNDO/S study, *Bull. Chem. Soc. Jpn.* 62 (1989) 1262–1268.
- [31] K. Hara, Z.S. Wang, T. Sato, A. Furube, R. Kato, H. Sugihara, Y. Dan-oh, C. Kasada, A. Shinpo, H. Arakawa, Oligothiophene containing coumarin dyes for efficient dye sensitized solar cells, *J. Phys. Chem. B* 109 (2005) 15476–15482.
- [32] K. Kalyanasundaram, M. Grätzel, Applications of functionalized transition metal complexes in photonic and optoelectronic devices, *Coord. Chem. Rev.* 177 (1998) 347–414.
- [33] S. Luzzati, M. Basso, M. Catellani, C.J. Brabec, D. Gebeyehu, N.S. Sariciftci, Photo-induced electron transfer from a dithieno thiophene-based polymer to TiO₂, *Thin Solid Films* 52–56 (2002) 403–404.
- [34] R. Argazzi, C.A. Bignozzi, T.A. Heimer, F.N. Castellano, G.J. Meyer, Enhanced spectral sensitivity from ruthenium(II) polypyridyl based photovoltaic devices, *Inorg. Chem.* 33 (1994) 5741–5749.
- [35] J. Jiu, S. Isoda, F. Wang, M. Adachi, *J. Phys. Chem. B* 110 (2006) 2087–2092.
- [36] R.Y. Ogura, S. Nakane, M. Morooka, M. Orihashi, Y. Suzuki, K. Noda, High-performance dye sensitized solar cell with a multiple dye system, *Appl. Phys. Lett.* 94 (2009), 073308-1-3.
- [37] J. Krüger, U. Bach, M. Grätzel, Modification of TiO₂ heterojunctions with benzoic acid derivatives in hybrid molecular solid-state devices, *Adv. Mater.* 12 (2000) 447–451.
- [38] K. Hara, H. Arakawa, Dye-sensitized Solar cells, in: A. Luque, S. Hegedus (Eds.), *Handbook of Photovoltaic Science and Engineering*, John Wiley and Sons Ltd, West Sussex, 2003, pp. 663–700.